Digital Droplet Loop-mediated Isothermal Amplification Featuring a Molecular Beacon Assay, 3D Printed Droplet Generation, and Smartphone Imaging for Sequence-specific DNA Detection

3 4 5

1

2

Shu-An Hsieh, Danial Shamsaei, Derek R. Eitzmann, and Jared L. Anderson*

6 7

Department of Chemistry, Iowa State University, Ames, Iowa, USA

8

Abstract

10 11

12

13

14

15

16

17 18

19

20

21

2223

24

25

26

27

28 29

30

31

9

Nucleic acid detection is widely used in the amplification and quantitation of nucleic acids from biological samples. While polymerase chain reaction (PCR) enjoys great popularity, expensive thermal cyclers are required for precise temperature control. Loop-mediated isothermal amplification (LAMP) enables highly sensitive, rapid, and low-cost amplification of nucleic acids at constant temperatures. LAMP detection often relies on double-stranded DNA binding dyes or metal indicators that lack sequence selectivity. Molecular beacons (MBs) are hairpin-shaped oligonucleotide probes whose sequence specificity in LAMP provides the capability of differentiating between single-nucleotide polymorphisms (SNPs). Digital droplet LAMP (ddLAMP) enables a large number of independent LAMP reactions to be performed and provides quantification of target DNA sequences. However, a major challenge with ddLAMP is the requirement of expensive droplet generators to form homogeneous microdroplets. In this study, we demonstrate for the first time that a 3D printed droplet generation platform can be coupled to a LAMP assay featuring MBs as sequence-specific probes. The low-cost 3D printed droplet generator system was designed and its customizability demonstrated in the formation of monodisperse ddLAMP assay-in-oil microdroplets. Additionally, a smartphone-based imaging system is demonstrated to increase accessibility for point-of-care applications. The MB-ddLAMP assay is shown to discriminate between two SNPs at various amplification temperatures to afford a useful platform for sequence-specific, sensitive, and accurate DNA quantification. This work expands the utility of MBs to ddLAMP for quantitative studies in the detection of SNPs and exploits the customizability of 3D printing technologies to optimize the homogeneity, size, and volume of oil-in-water microdroplets.

32 33

34

*Corresponding Author:

- 35 Jared L. Anderson
- 36 Department of Chemistry
- 37 Iowa State University
- 38 1605 Gilman Hall
- 39 Ames, IA 50011
- 40 Email: andersoj@iastate.edu

41

Introduction

Nucleic acid detection (NAD) methods, such as the polymerase chain reaction (PCR), are used in the detection of DNA or RNA from biological samples. ^{1,2} Traditionally, real-time PCR is employed in high throughput assays within clinical settings to detect and quantify the concentration of target DNA fragments. ³ However, real-time PCR requires expensive equipment capable of precise thermal cycling and amplicon detection, ⁴ thereby significantly reducing its practicality in resource-limited settings. Recently, several isothermal amplification methods, such as recombinase polymerase amplification (RPA), ⁵ nucleic acid sequence-based amplification (NASBA), ⁶ isothermal multiple-self-matching-initiated amplification (IMSA), ⁷ rolling circle amplification (RCA), ⁸ and loop-mediated isothermal amplification (LAMP) have been used to circumvent PCR thermal cycling requirements. Among these, LAMP generally exhibits shorter amplification times compared to PCR and is robust, while also being tolerant to salts. ¹⁰ LAMP is performed at a constant temperature (60 to 65 °C) and typically requires 4-6 primers to amplify a target DNA sequence. ¹¹ Amplification under isothermal conditions eliminates the use of sophisticated equipment and can be readily adapted for use in less developed areas. ¹²

LAMP detection methods often involve the use of metal indicators such as calcein,¹³ double-stranded fluorescent DNA binding dyes such as Eva Green,¹⁴ sequence-specific probes including molecular beacons (MB)¹⁵⁻¹⁷ and scorpion primers.¹⁸ While nonspecific dyes are not able to distinguish between single-nucleotide polymorphisms (SNPs), MBs have been shown to be selective in SNP discrimination.¹⁵ SNPs involve a single nucleotide difference at a specific position within two otherwise identical nucleic acid sequences. SNPs are among the most common genetic variations found within the human genome and are correlated with various diseases and drug efficacy.¹⁹⁻²¹ Therefore, sequence-specific detection methods are needed to provide early

diagnosis of illnesses caused by SNPs and play a critical role in the development of ideal treatment protocols.²²

Digital nucleic acid detection (dNAD) methods provide highly sensitive and accurate absolute quantification of nucleic acids compared to traditional detection methods.²³ dNAD approaches can typically be divided into chip²⁴ and droplet-based methods.^{25, 26} Chip-based methods are often more time-consuming due to complicated fabrication processes required in the manufacturing of microfluidic chips.²⁷ In addition, there are often limitations in the number of reactions (~1,000 microwells) that can be performed on-chip.²⁸ However, droplet-based dNAD is much simpler, faster, and requires a droplet generator to produce more than 10,000 pico-liter sized droplets in a short period of time.²⁹ The massive number of droplets and their size enables droplet-based dNAD (ddNAD) approaches to achieve more accurate DNA quantification.³⁰

Previous studies by our group have used LAMP to qualitatively study MBs as sequence-specific probes at reaction volumes of 20 μL, where allelic discrimination was achieved for wild-type and mutant BRAF V600E. Wan and co-workers developed a digital microfluidic on-chip system implementing both a non-sequence specific fluorescence dye and MB. Reduced false-positive LAMP reactions within a 1 μL droplet-size reactor were demonstrated; however, absolute quantification was not investigated. Tan *et al.* reported a microfluidic chip system as droplet generator for ddLAMP with scorpion-shaped probes to detect SNPs within a target DNA sequence. While selective, these probes are considerably more expensive and complicated to design compared to MBs. ddLAMP techniques have been carried out in several platforms that use commercial droplet generators, membranes, and PDMS microfluidic chips to produce droplets. However, these approaches can be costly and often require specialized equipment or facilities. Recently, rapid prototyping using 3D printing has increased significantly due to its

simplicity, customizability, speed, and cost-effectiveness. 3D printed micro/milli-fluidic devices have accelerated fabrication processes and can be carried out using commercial benchtop 3D printers. Studies utilizing MBs for SNP detection in a ddLAMP format where 3D printed devices are used to generate water-in-oil microdroplets has yet to be achieved.

In this study, we demonstrate the development of a ddLAMP assay featuring MB as a sequence-specific fluorescent probe coupled to a cost-effective 3D printed milli-fluidic droplet generation system. The sequence-specific ddLAMP approach is used in the quantitation of the OmpW gene from Vibrio cholera and a SNP-modified OmpW template in which the OmpW+SNP sequence is a synthetic sequence used to show MB sequence specificity, as demonstrated previously. 15 Characteristics and performance of the 3D droplet generation system were evaluated based on the size and homogeneity of the formed droplets. Secondly, a smartphone-imaging system is demonstrated to increase accessibility of the ddLAMP technique and enable a comparison of quantitative results to a fluorescence microscope. In addition to investigating the optimal MB concentration yielding the highest SNP specificity, the fluorescence intensities of droplets were extracted by Fiji software and compared for MB-ddLAMP assays containing different MB concentration. A MATLAB code permits the total number of droplets and positive droplets to be counted by collecting fluorescence images of the droplets obtained from MBddLAMP assays with varied input DNA concentration. Lastly, the relationship between actual and calculated copy number ratio of OmpW to OmpW+SNP DNA templates based on the fraction of fluorescent droplets was investigated.

110

111

112

90

91

92

93

94

95

96

97

98

99

100

101

102

103

104

105

106

107

108

109

Experimental

Materials and Reagents

Deoxynucleotide triphosphates (dNTPs), isothermal amplification buffer (10X), MgSO₄, and *Bst* 2.0 Warmstart DNA polymerase were purchased from New England Biolabs (Ipswich, MA, USA). A plasmid (3.9 kb) containing the 222 bp OmpW gene sequence was obtained from Eurofins Genomics (Louisville, KY, USA). DNA sequences for the OmpW gBlockTM gene fragment, OmpW+SNP gBlockTM gene fragment, molecular beacon, and all primers for LAMP were purchased from Integrated DNA Technologies (Coralville, IA, USA) and are shown in Table S1. Deionized water (18.2 MΩ cm) was obtained from a Millipore Milli-Q water purification system (Bedford, MA, USA). Isopropanol (IPA, 99% HPLC grade) was purchased from Sigma-Aldrich (St. Louis, MO, USA). DNA LoBind® Tubes were purchased from Eppendorf Inc. (Hamburg, Germany). Polyether ether ketone (PEEK) tubing with an outer diameter (OD) of 1/16" and an inner diameter (ID) of 0.005" was purchased from Restek Corporation (Bellefonte, PA, USA). PEEKsilTM tubing with an OD of 1/16" and an ID of 0.005" was purchased from Sigma-Aldrich.

Fabrication of 3D printed millifluidic droplet generator

The 3D printed droplet generator used in this work, shown in Figure S1, was designed by Inventor Professional 2020 Student Edition developed by Autodesk Inc. (San Rafael, CA, USA). The droplet generator consists of a Y-junction channel with a channel height of 1.0 mm, two 1.2 mm ID inlet channels, and one 1.85 mm ID outlet channel. The designed model was printed by a Form3 stereolithography 3D printer using clear resin (FLGPCL04) purchased from Formlabs (Somerville, MA, USA). After printing, the droplet generator was subjected to a 10 minute IPA wash in Form Wash (Somerville, MA, USA). To prevent residual resin being left in the channels, it was flushed with IPA for 10 seconds using a Golander peristaltic pump (Norcross, GA, USA), followed by application of high pressure air flow through the channels to remove any remaining

IPA. The printed droplet generator was then placed in Form Cure (Somerville, MA, USA) for a UV/thermal curing step at 60 °C for 60 minutes.

Setup of droplet generation system

Two inlets of the droplet generator were each connected to a silicon tube (Quickun, Australia) with dimensions of 1.0 mm OD 0.5 x mm ID and length of 4 cm. The ddLAMP assay inlet was connected to a 100 μ L syringe purchased from Hamilton Inc. (Houston, TX, USA), and the inlet for the oil phase was connected to a 1 mL Hamilton syringe. Each syringe was placed on separate Harvard Apparatus 11 Plus syringe pumps (Holliston, Ma, USA) for precise flow rate control. The outlet of the droplet generator was connected to a 15 cm long segment of PEEK tubing with an OD of 1/16" and an ID of 0.005", and the connection sealed using a 1.0 mm ID x 2.0 mm OD silicon tube of 0.5 cm length.

MB-ddLAMP assay conditions

Before beginning any experiments, all pipettes, the droplet generation system, and the working spaces were all thoroughly cleaned with 10% diluted bleach and DI water to prevent any possible contamination. A 50 μL volume of the MB-ddLAMP assay was prepared in 1 mL DNA LoBind[®] Tubes. The assay consisted of 1.4 mM dNTPs, 6 mM MgSO₄, isothermal amplification buffer (1X), 1.6 μM FIP, 1.6 μM BIP, 0.2 μM F3, 0.2 μM B3, 0.4 μM LF, 0.7 μM MB, 0.32 U/μL *Bst* 2.0 WarmStart DNA polymerase, and 5 μL of OmpW/OmpW+SNP DNA template. An orthogonal assay is demonstrated using a fluorescence dye, 1X EvaGreen, to ensure amplification of the OmpW and OmpW+SNP DNA templates, as shown in Figure S2. The assay was centrifuged for 15 seconds, followed by a 30 second vortex step. A 10 μL volume of the assay was then pipetted into a qPCR tube (0.1 mL) for end-point fluorescence detection. All isothermal amplification studies were carried out using a CFX Touch real-time PCR detection system from Bio-Rad

Laboratories (Hercules, CA, USA) at 65 °C for 60 minutes to reach the maximum fluorescence intensity, as shown in Figure S3.

Droplet generation procedure

Before each sample was applied to the system, 100 μL of DI water was injected 2 times to rinse the channels and prevent cross contamination between samples. As shown in Figure 1, the remainder of the MB-ddLAMP assay was filled into a 100 μL gastight syringe and placed onto the syringe pump. A 1 mL syringe then was filled with QX200TM droplet generation oil (Bio-Rad) and placed onto the other syringe pump. A ddLAMP assay-to-oil flow rate ratio of 1:8 was chosen, and flow of both syringes was commenced simultaneously. A 0.2 mL PCR tube purchased from Thermo Fisher Scientific (Waltham, MA, USA) was used to capture the generated droplets at the outlet followed by careful transfer to qPCR tubes for subsequent isothermal amplification.

Smartphone-based fluorescence imaging system

A smartphone-based imaging system, shown in Figure 2, is comprised of a smartphone (IPhone 13 Pro), a 4x plan achromatic microscopic objective from Labomed Inc. (Los Angeles, CA, USA), a 550 nm long pass filter, and a transilluminator obtained from Pearl Biotech (Kvistgaard, Denmark). In addition, the entire system was assembled using 3D printed parts designed in Autodesk Inventor modeling software (San Rafael, CA, USA) and printed by an Ultimaker S5 printer (Utrecht, Netherlands) using black polylactic acid (PLA) filament (2.85 mm diameter).

Fluorescence imaging and image processing

The amplified droplets were carefully pipetted into the EveTM cell counting slides, purchased from NanoEntek (Seoul, South Korea). A fluorescence image was first taken by the smartphone-based imaging system, followed by a Zeiss Axioplan II fluorescence microscope

(Jena, Germany) equipped with digital cameras. For each sample imaged by fluorescence microscopy, a total of thirty-five images were obtained and stitched into a full-view image to cover a chamber of droplets pipetted into the cell counting slides, as shown in Figure S4. The stitched image was then saved as a raw image for further analysis. For smartphone imaging, brightfield and fluorescence images of each sample were taken to determine the total number of droplets and positive droplets, respectively. The sequence of all image processing procedures is detailed in Figure S5. All images were processed using open-source Fiji software to obtain the relative fluorescence intensity and diameter of each droplet. A customized MATLAB script was then applied to obtain the total number of counted droplets, number of positive droplets, distribution of relative fluorescence intensity, average relative fluorescence intensity of positive droplets, and fraction of positive droplets.

Statistical data analysis

In ddLAMP studies, the bulk MB-ddLAMP assay is randomly emulsified into ten thousand or more droplets. The partitioned droplets can be classified into negative droplets that lack DNA template complementary to the MB and positive droplets that contain target DNA template. A threshold was set using the highest relative fluorescence intensity from the droplets generated with the no-template control (NTC) assay. Droplets were designated as positive when the relative fluorescence intensity was above the threshold. After isothermal amplification, a fraction of positive droplets was observed using fluorescence microscopy. In this study, approximately 10,000 droplets were analyzed per assay. The estimated DNA concentration was calculated using the Poisson distribution model. An assumption of random distribution of DNA into the droplets was applied for the ddLAMP technique when all droplets were formed homogenously. Therefore, by

using the Poisson distribution, the probability of copies of target droplet DNA can be represented by Eq 1.

206 probability(k) =
$$\frac{\lambda^k}{k!}e^{-\lambda}$$
 (Eq. 1)

where k is the probability of copies of target droplet DNA per droplet and λ is the average number of target DNA (copies/droplets). E represents the percentage of negative droplets and the probability of negative droplet is E = probability(0) = $e^{-\lambda}$.

$$\lambda = -\ln\left(E\right) = -\ln\left(\frac{\text{\# of negative droplets}}{\text{\# of total droplets}}\right) = -\ln\left(1 - \frac{P}{T}\right) \left(\frac{\text{copies}}{\text{droplet}}\right) \tag{Eq. 2}$$

- 211 Calculation of the actual DNA concentration, known as the input DNA concentration, and the
- 212 DNA concentration based on the droplet images can be performed using Eqs. 3 and 4,

213 Actual DNA concentration
$$\left(\frac{copies}{\mu L}\right) = \frac{Copies\ of\ DNA}{Assay\ volume\ (\mu L)}$$
 (Eq. 3)

214 Calculated DNA concentration
$$\left(\frac{copies}{\mu L}\right) = \frac{-ln\left(1 - \frac{P}{T}\right)\left(\frac{copies}{droplet}\right)}{Droplet \ volume\left(\frac{\mu L}{droplet}\right)}$$
 (Eq. 4)

where the number of DNA copies was determined from the DNA molar mass and the input DNA concentration of the OmpW DNA sequence, P is the number of positive droplets, T is the total number of droplets, and the ratio $(\frac{P}{T})$ is the fraction of positive droplets. Both P and T were obtained from fluorescence image analysis. The droplets are assumed to be spherical; therefore, the droplet volume was calculated using the volume of a sphere (droplet volume $(\mu L) = \frac{4}{3}\pi x$ $(\frac{average\ feret\ diameter}{2})^3 (m) x 10^3)$, where the average feret diameter is obtained from Fiji software. However, due to the 100 μ m height limitation of the imaging slides, the droplet volume was calculated using the volume of an ellipsoid (droplet volume $(\mu L) = \frac{4}{3}\pi x \le 10^{-6} x$ $(\frac{average\ feret\ diameter}{2})^2 (m) x 10^3)$ when the average feret diameter exceeded 100 μ m.

225

226

227

228

229

230

231

232

233

234

235

236

237

238

239

240

241

242

243

244

245

246

Results and Discussion

Design and fabrication of 3D printed millifluidic droplet generation system

A customized 3D printed millifluidic droplet generation system was designed in this study to perform ddLAMP. All components were optimized using suitable tubing dimensions and connections to form stable ddLAMP assay-in-oil microdroplets, as shown in Figure 1. While a commercial droplet generator can cost more than 100,000 USD, the generator and components used in this study were purchased for less than 1,000 USD. Customizability of 3D printing provides enormous flexibility in choosing different channel dimensions, syringe volumes, and compatibility with other platforms. A droplet generator featuring a Y-junction consisting of two inlet channels and one outlet channel, shown in Figure S1, was used in this study. One inlet was used to introduce the ddLAMP assay as the dispersed phase while the other inlet was used for the continuous phase. The outlet channel was interfaced with PEEK tubing (0.005") to facilitate the formation of miniature droplets. A key requirement for the formation of homogenous droplets is the creation of a leak-free system requiring air-tight sealing of all connections. The elasticity of silicon tubes was found to be superior to epoxy glue in preventing leaks at all connections. Smoothness of the PEEK tubing interface was also observed to affect droplet homogeneity where rough surfaces were observed to interrupt droplet formation, resulting in greater droplet diameter polydispersity. To circumvent this, sandpaper was used to smoothen these surfaces.

Performance of 3D printed droplet system

Studies have shown that the inner channel surface hydrophobicity can affect the stability of formed droplets.³⁷ PEEK tubing featuring a hydrophobic inner surface and PEEKsilTM hydrophilic inner surface tubing were studied as outlet tubing materials. PEEKsilTM tubing consists

of an additional fused silica coating layer and is commonly used to create a hydrophilic surface layer (Figure S6(a) and (b)). Application of the hydrophobic PEEK tubing resulted in the formation of monodisperse droplets whereas a mixture of polydisperse droplets was observed using PEEKsilTM tubing, as shown in Figure S6(c) and (d). The monodisperse emulsion can be attributed to a higher contact angle of the water droplets with the hydrophobic surface. Based on these data, the hydrophobic inner surface was chosen for the generation of droplets throughout this study.

An underlying assumption of ddLAMP is based on the random distribution of target DNA into the droplets followed by DNA amplification. Therefore, droplet size homogeneity is critical to obtain accurate and precise ddLAMP results due to the equal probability of DNA copies being distributed into droplets. The distribution of droplet diameters before and after isothermal amplification was investigated. As shown in Figure S7(a), an average droplet diameter of 94.2 μ m with a relative standard deviation (RSD) of 5.94 % was found within a set of generated droplets prior to isothermal amplification. Following isothermal amplification at 65 °C, the average droplet diameter increased slightly to 95.1 μ m (RSD of 4.74 %), as shown in Figure S7(b), demonstrating that droplet sizes remained uniform after ddLAMP.

Droplet size is known to play a critical role in droplet stability and the DNA concentration range that can be determined by ddLAMP. ³⁸ Several factors including the viscosity of ddLAMP assay/oil solution, ³⁹ total pressure added through the channels, ⁴⁰ and flow rate ratio ⁴¹ of ddLAMP assay and oil can influence the size of droplets. Therefore, droplet size customizability using 3D printing makes it feasible to optimize conditions while applying different types of oil and ddLAMP assay. In this study, various flow rate ratios of ddLAMP assay-to-oil (e.g., 1:2, 1:4, 1:6, 1:8) were investigated to evaluate the sizes of formed droplets. As shown in Figure 3, when the oil flow rate was increased to eight times the assay flow rate, the average droplet diameter increased from 95.0

 \pm 1.5 µm to 179.0 \pm 3.7 µm. Since smaller droplets allow for more accurate ddLAMP results and enhanced droplet stability,^{38, 42} a ddLAMP assay-to-oil flow rate ratio of 1:8 was used to generate droplets for quantitative studies.

Optimization of MB-ddLAMP assay using OmpW plasmid versus $gBlock^{TM}$ gene fragment as DNA template

To enhance the accuracy of ddLAMP, discrimination between negative and positive droplets based on their relative fluorescence intensity is crucial. A 3.9 kb plasmid containing the 222 bp OmpW gene insert and a 222 bp gBlockTM OmpW gene fragment were tested in this study. As shown in Figure S8(a), results from end-point LAMP did not show a significant difference in the fluorescence intensity between the two DNA templates. The same two sets of assays were also subjected to ddLAMP, where the distribution of droplets based on their fluorescence intensities did not reveal a significant difference in positive droplets among the sets of assays, as shown in Figure S8(b).

Concentration of molecular beacon in ddLAMP assay

Since MBs are employed as a fluorescence probe in the LAMP assay to achieve sequence-specific differentiation, optimizing their concentration is important as it may affect the observed fluorescence intensity difference between negative and positive droplets. While higher MB concentration levels are expected to increase the observed fluorescence of positive droplets, operating at excessively high MB concentration levels can result in a slight decrease in the discrimination of fluorescence droplets for the ddLAMP assay. This can be due to the higher background fluorescence intensity caused by the negative droplets, as shown in Figure S9. In this study, three MB-ddLAMP assays containing MB concentrations of 0.3 μ M, 0.5 μ M, and 0.7 MB

were investigated to examine the relative fluorescence intensity obtained from a 10 μ L end-point LAMP assay and fluorescence intensities of all positive droplets after ddLAMP. From Figure S9(a) and (b), increased fluorescence was observed from both the end-point LAMP and ddLAMP assays. The assay containing 0.7 μ M MB exhibited the highest relative fluorescence intensity using end-point LAMP as well as high values for positive droplets using ddLAMP. Since highly fluorescent positive droplets were observed at this concentration, it was used to perform all quantitative sequence-specific measurements in this study.

Sequence-specific nucleic acid detection using MB-ddLAMP

293

294

295

296

297

298

299

300

301

302

303

304

305

306

307

308

309

310

311

312

313

314

315

Previous studies developed a colorimetric method by incorporating hydoxynaphthol blue dye and MBs into a 10 µL LAMP assay to demonstrate sequence-selective detection between the OmpW and OmpW+SNP sequences. 15 Amplification temperature is an important factor in SNP detection and can be determined using annealing profiles that probe the stability of MB binding to the SNP sequence. An optimal SNP detection temperature will result in the largest difference in fluorescence intensities between the OmpW and OmpW+SNP sequences. An amplification temperature of 65 °C was previously shown to yield the best performance in SNP detection using the same sequences in a 10 µL bulk LAMP assay; however, the optimal amplification temperature for ddLAMP has yet to be studied. Three different temperatures, namely, 64 °C, 65 °C, and 66 °C were investigated. At each amplification temperature, OmpW and OmpW+SNP sequences at a concentration of 4,390 copies/µL of the reaction were added into two separate tubes. End-point fluorescence results in Figure S10(a) show that significant fluorescence was obtained for both endpoint LAMP and MB-ddLAMP in the presence of OmpW template while the fluorescence was diminished in both end-point LAMP and MB-ddLAMP when the OmpW template was replaced with the OmpW+SNP template. The decreased fluorescence of OmpW+SNP assays can be

attributed to weaker interactions between MB and the OmpW+SNP template. Similarly, discrimination between negative and positive droplets was not observed for the OmpW+SNP assay at the three temperatures examined, as shown in Figure S10(b). Conversely, MB-ddLAMP assays containing the OmpW sequence show a clear discrimination between negative and positive droplets at all temperatures, indicating that SNP detection can be achieved due to the absence of fluorescent droplets when the assay contains only OmpW+SNP DNA template. The average fluorescence intensities after isothermal amplification at 64 °C, 65 °C, and 66 °C are shown in Figure S10. An isothermal amplification temperature of 65 °C yielded the highest fluorescence intensity for positive droplets and the best discrimination of OmpW and OmpW+SNP sequences.

Comparison of smartphone-based system and fluorescence microscope

To perform SNP quantification using MB-ddLAMP, the standard curve for assays containing only OmpW template was first investigated. Assays containing OmpW DNA template at concentrations ranging from 4.39, 43.9, 4390, and 43,900 copies/μL of the reaction were tested. All assays were imaged by both the smartphone-based imaging system and fluorescence microscope. At least 10,000 droplets were generated and counted based on their fluorescence intensity distribution where the results show that the fraction of positive droplets rises incrementally as the DNA concentration is increased. Additionally, the MB-ddLAMP system can detect DNA concentrations as low as 4.39 copies/μL of the reaction, providing comparable or better sensitivity compared to recent sequence-specific LAMP detection methods, which typically produce detection limits down to 2-250 copies/μL of the reaction. 15,43,44,45

As shown in Figure S11(b), the fraction of positive droplets can be correlated to the actual DNA concentration within the MB-ddLAMP assay. Moreover, the fraction of positive droplets can be applied to the Poisson distribution and the calculated DNA concentration obtained using

Eq. 4. A linear relationship between the actual DNA concentration versus the calculated DNA concentration can be observed (Figure S11 (c)) and reveals that the calculated concentration deviates further from the actual DNA concentration with increasing amount of input DNA. This can be attributed to various systematic errors including heterogenous distribution of target DNA in the assay and droplet coalescence. A linear equation shown within Figure S11 can be obtained and aids in accurately quantifying higher concentrations of DNA, permitting the actual DNA concentration to be obtained by analyzing the fraction of positive droplets. As shown in Table S2 and Figure S11, the calculated DNA concentration from the images taken by the smartphone imaging system were comparable to the images taken from the fluorescence microscope.

Investigation of OmpW and OmpW+SNP DNA template copy number ratio in MB-ddLAMP

To test the detection capability of MB-ddLAMP for target DNA in the presence of interfering DNA, different copy number ratios of OmpW to OmpW+SNP sequences were investigated. A final reaction concentration of 4,390 copies/µL of OmpW and OmpW+SNP sequences were added to all assays. An increase in the OmpW to OmpW+SNP ratio resulted in a larger fraction of positive droplets being observed, as shown in Figure 4(a,b). The assay is able to detect OmpW to OmpW+SNP ratios down to 1 %. The actual and calculated ratio of OmpW to OmpW+SNP sequences can be determined using Eqs. 5 and 6:

358 Actual ratio of
$$OmpW$$
 to $OmpW + SNP$ sequence = $\frac{Concentration of OmpW}{Concentration of total DNA}$ (Eq. 5)

Calculated ratio of OmpW to OmpW + SNP sequence =
$$\frac{\frac{P}{T}}{\frac{P}{T} \text{ of } 100\% \text{ OmpW}}$$
 (Eq. 6)

where P is the number of positive droplets, T is the total number of droplets, $\frac{P}{T}$ is the fraction of positive droplets obtained from the tested assay and $\frac{P}{T}$ of 100 % OmpW is obtained from average fraction of positive droplets from triplicates of MB-ddLAMP containing only OmpW sequence. As shown in Figure 4(c), the linear relationship (R² = 0.9972) demonstrates agreement between the calculated and actual ratios of OmpW to OmpW+SNP DNA templates over several orders of magnitude.

Conclusions

In this work, a MB capable of achieving high single-nucleotide selectivity was coupled with ddLAMP to perform quantification of the OmpW and OmpW+SNP sequences using a 3D printed millifluidic droplet generation device. The droplet generating device was capable of forming homogeneous droplets while enabling the droplet diameter to be customized. A droplet generation system and smartphone-based imaging system were developed and coupled in this study to significantly lessen the cost of performing ddLAMP and can be used in resource-limited settings to perform ddNAD. The MB-ddLAMP approach enabled quantification of input OmpW DNA template based on the observed number of fluorescent droplets, providing detection limits of OmpW template down to 4.39 copies/µL of the reaction. Furthermore, copy number ratios of OmpW to OmpW+SNP DNA down to 1 % could be detected. The development of a MB-ddLAMP assay capable of SNP discrimination is very important for clinical diagnostics, biomedicine, and forensics research where it is desired to measure allele abundance down to the single copy number. While this study demonstrates a proof-of-concept platform for MB-ddLAMP, future work will involve multiplexed detection of SNP sequences using MBs and consolidation of the droplet

generation system with a heating and detection system in order to minimize loss of DNA and increase efficiency of the ddLAMP process.

Acknowledgement

- 386 J.L.A. acknowledges funding from the Chemical Measurement and Imaging Program at the
- National Science Foundation (Grant No. CHE-2203891). J.L.A. and S.H. thank the Alice Hudson
- 388 Professorship for support.

Supporting Information

List of primers, sequences of MB and DNA template used, ddLAMP quantification comparison between fluorescence microscopy and smartphone-based imaging, 3D-printed droplet generator models, orthogonal assay using EvaGreen fluorescent dye, procedures used for image processing, stitched image of fluorescent droplets, images highlighting the cross-section of PEEK and PEEKsilTM tubing, droplet distribution before and after isothermal amplification, comparison of relative fluorescence intensity plots for end-point LAMP using plasmid versus gene fragment DNA template, fluorescence intensity plots as a function of MB concentration for end-point LAMP and ddLAMP, plots of end-point LAMP for SNP detection, and statistical analysis of MB-ddLAMP as a function of OmpW concentration using fluorescence microscopy and smartphone-based imaging system are provided.

References

- 403 1. Schochetman, G.; Ou, C.-Y.; Jones, W. K., Polymerase chain reaction. *J. Infect. Dis.*
- **1988,** *158* (6), 1154-1157.
- 405 2. Erlich, H. A., Polymerase chain reaction. *J. Clin. Immunol.* **1989,** 9 (6), 437-447.

- Wilhelm, J.; Pingoud, A., Real-time polymerase chain reaction. *Chembiochem* **2003**, *4*
- 407 (11), 1120-1128.
- 408 4. Kubista, M.; Andrade, J. M.; Bengtsson, M.; Forootan, A.; Jonák, J.; Lind, K.;
- 409 Sindelka, R.; Sjöback, R.; Sjögreen, B.; Strömbom, L., The real-time polymerase chain
- 410 reaction. Mol. Aspects Med. 2006, 27 (2-3), 95-125.
- Daher, R. K.; Stewart, G.; Boissinot, M.; Bergeron, M. G., Recombinase polymerase
- amplification for diagnostic applications. Clin. Chem. 2016, 62 (7), 947-958.
- 413 6. Deiman, B.; van Aarle, P.; Sillekens, P., Characteristics and applications of nucleic acid
- sequence-based amplification (NASBA). Mol. Biotechnol. 2002, 20 (2), 163-179.
- Ding, X.; Wu, W.; Zhu, Q.; Zhang, T.; Jin, W.; Mu, Y., Mixed-dye-based label-free
- and sensitive dual fluorescence for the product detection of nucleic acid isothermal multiple-self-
- 417 matching-initiated amplification. *Anal. Chem.* **2015**, *87* (20), 10306-10314.
- 418 8. Ali, M. M.; Li, F.; Zhang, Z.; Zhang, K.; Kang, D.-K.; Ankrum, J. A.; Le, X. C.;
- 219 Zhao, W., Rolling circle amplification: a versatile tool for chemical biology, materials science
- 420 and medicine. Chem. Soc. Rev. 2014, 43 (10), 3324-3341.
- 421 9. Notomi, T.; Mori, Y.; Tomita, N.; Kanda, H., Loop-mediated isothermal amplification
- 422 (LAMP): principle, features, and future prospects. J. Microbiol. 2015, 53 (1), 1-5.
- 423 10. Notomi, T.; Okayama, H.; Masubuchi, H.; Yonekawa, T.; Watanabe, K.; Amino, N.;
- Hase, T., Loop-mediated isothermal amplification of DNA. *Nucleic Acids Res.* **2000**, *28* (12),
- 425 e63-e63.
- 426 11. Nagamine, K.; Hase, T.; Notomi, T., Accelerated reaction by loop-mediated isothermal
- 427 amplification using loop primers. *Mol. Cell. Probes* **2002**, *16* (3), 223-229.

- 428 12. Nzelu, C. O.; Kato, H.; Peters, N. C., Loop-mediated isothermal amplification (LAMP):
- 429 An advanced molecular point-of-care technique for the detection of Leishmania infection. *PLoS*
- 430 Negl. Trop. Dis. **2019**, 13 (11), e0007698.
- 431 13. Tomita, N.; Mori, Y.; Kanda, H.; Notomi, T., Loop-mediated isothermal amplification
- 432 (LAMP) of gene sequences and simple visual detection of products. *Nat. Protoc.* **2008**, *3* (5),
- 433 877-882.
- 434 14. Oscorbin, I. P.; Belousova, E. A.; Zakabunin, A. I.; Boyarskikh, U. A.; Filipenko, M.
- 435 L., Comparison of fluorescent intercalating dyes for quantitative loop-mediated isothermal
- 436 amplification (qLAMP). *Biotechniques* **2016**, *61* (1), 20-25.
- 437 15. Varona, M.; Anderson, J. L., Visual Detection of Single-Nucleotide Polymorphisms
- 438 Using Molecular Beacon Loop-Mediated Isothermal Amplification with Centrifuge-Free DNA
- 439 Extraction. Anal. Chem. 2019, 91 (11), 6991-6995.
- 440 16. Varona, M.; Eitzmann, D. R.; Pagariya, D.; Anand, R. K.; Anderson, J. L., Solid-Phase
- 441 Microextraction Enables Isolation of BRAF V600E Circulating Tumor DNA from Human
- Plasma for Detection with a Molecular Beacon Loop-Mediated Isothermal Amplification Assay.
- 443 Anal. Chem. **2020**, 92 (4), 3346-3353.
- 444 17. Varona, M.; Eitzmann, D. R.; Anderson, J. L., Sequence-Specific Detection of ORF1a,
- BRAF, and ompW DNA Sequences with Loop Mediated Isothermal Amplification on Lateral
- Flow Immunoassay Strips Enabled by Molecular Beacons. *Anal. Chem.* **2021,** *93* (9), 4149-4153.
- 18. Thelwell, N.; Millington, S.; Solinas, A.; Booth, J.; Brown, T., Mode of action and
- 448 application of Scorpion primers to mutation detection. *Nucleic Acids Res.* **2000**, 28 (19), 3752-
- 449 3761.

- 450 19. Lin, Y.-W.; Ho, H.-T.; Huang, C.-C.; Chang, H.-T., Fluorescence detection of single
- nucleotide polymorphisms using a universal molecular beacon. *Nucleic Acids Res.* **2008**, *36* (19),
- 452 e123-e123.
- 453 20. Zou, Z.; Qing, Z.; He, X.; Wang, K.; He, D.; Shi, H.; Yang, X.; Qing, T.; Yang, X.,
- 454 Ligation-rolling circle amplification combined with γ-cyclodextrin mediated stemless molecular
- beacon for sensitive and specific genotyping of single-nucleotide polymorphism. *Talanta* **2014**,
- 456 *125*, 306-312.
- 457 21. Collins, F. S.; Guyer, M. S.; Chakravarti, A., Variations on a theme: cataloging human
- 458 DNA sequence variation. *Science* **1997**, *278* (5343), 1580-1581.
- 459 22. Marth, G. T.; Korf, I.; Yandell, M. D.; Yeh, R. T.; Gu, Z.; Zakeri, H.; Stitziel, N. O.;
- Hillier, L.; Kwok, P.-Y.; Gish, W. R., A general approach to single-nucleotide polymorphism
- 461 discovery. *Nat. Genet.* **1999**, *23* (4), 452-456.
- 462 23. Vogelstein, B.; Kinzler, K. W., Digital PCR. Pro. Natl. Acad. Sci. 1999, 96 (16), 9236-
- 463 9241.
- 464 24. Wu, Z.; Bai, Y.; Cheng, Z.; Liu, F.; Wang, P.; Yang, D.; Li, G.; Jin, Q.; Mao, H.;
- Zhao, J., Absolute quantification of DNA methylation using microfluidic chip-based digital
- 466 PCR. Biosens. Bioelectron. 2017, 96, 339-344.
- 467 25. Hindson, C. M.; Chevillet, J. R.; Briggs, H. A.; Gallichotte, E. N.; Ruf, I. K.; Hindson,
- 468 B. J.; Vessella, R. L.; Tewari, M., Absolute quantification by droplet digital PCR versus analog
- 469 real-time PCR. *Nat. Methods* **2013**, *10* (10), 1003-1005.
- 470 26. Yuan, H.; Chao, Y.; Shum, H. C., Droplet and Microchamber-Based Digital Loop-
- 471 Mediated Isothermal Amplification (dLAMP). Small 2020, 16 (9), 1904469.

- 472 27. Barbulovic-Nad, I.; Yang, H.; Park, P. S.; Wheeler, A. R., Digital microfluidics for cell-
- 473 based assays. *Lab Chip* **2008**, *8* (4), 519-526.
- 474 28. Sundberg, S. O.; Wittwer, C. T.; Gao, C.; Gale, B. K., Spinning disk platform for
- 475 microfluidic digital polymerase chain reaction. *Anal. Chem.* **2010**, 82 (4), 1546-1550.
- 476 29. Li, N.; Ma, J.; Guarnera, M. A.; Fang, H.; Cai, L.; Jiang, F., Digital PCR quantification
- of miRNAs in sputum for diagnosis of lung cancer. J. Cancer Res. Clin. Oncol. 2014, 140 (1),
- 478 145-150.
- 479 30. Pinheiro, L. B.; Coleman, V. A.; Hindson, C. M.; Herrmann, J.; Hindson, B. J.; Bhat,
- 480 S.; Emslie, K. R., Evaluation of a droplet digital polymerase chain reaction format for DNA copy
- 481 number quantification. *Anal. Chem.* **2012,** *84* (2), 1003-1011.
- 482 31. Wan, L.; Chen, T.; Gao, J.; Dong, C.; Wong, A. H.-H.; Jia, Y.; Mak, P.-I.; Deng, C.-
- 483 X.; Martins, R. P., A digital microfluidic system for loop-mediated isothermal amplification and
- sequence specific pathogen detection. Sci. Rep. 2017, 7 (1), 1-11.
- 485 32. Tan, Y.-L.; Huang, A.-Q.; Tang, L.-J.; Jiang, J.-H., Multiplexed droplet loop-mediated
- 486 isothermal amplification with scorpion-shaped probes and fluorescence microscopic counting for
- digital quantification of virus RNAs. Chem. Sci. 2021, 12, 8445-8451.
- 488 33. Hu, Y.; Xu, P.; Luo, J.; He, H.; Du, W., Absolute Quantification of H5-Subtype Avian
- 489 Influenza Viruses Using Droplet Digital Loop-Mediated Isothermal Amplification. Anal. Chem.
- **2017,** *89* (1), 745-750.
- 491 34. Lin, X.; Huang, X.; Urmann, K.; Xie, X.; Hoffmann, M. R., Digital Loop-Mediated
- 492 Isothermal Amplification on a Commercial Membrane. ACS Sens. 2019, 4 (1), 242-249.

- 493 35. Ma, Y.-D.; Luo, K.; Chang, W.-H.; Lee, G.-B., A microfluidic chip capable of
- 494 generating and trapping emulsion droplets for digital loop-mediated isothermal amplification
- 495 analysis. Lab Chip **2018**, 18 (2), 296-303.
- 496 36. Basu, A. S., Digital Assays Part I: Partitioning Statistics and Digital PCR. SLAS Technol.
- **2017,** *22* (4), 369-386.
- 498 37. Yoshimitsu, Z.; Nakajima, A.; Watanabe, T.; Hashimoto, K., Effects of Surface
- 499 Structure on the Hydrophobicity and Sliding Behavior of Water Droplets. *Langmuir* **2002**, *18*
- 500 (15), 5818-5822.
- 501 38. Košir, A. B.; Divieto, C.; Pavšič, J.; Pavarelli, S.; Dobnik, D.; Dreo, T.; Bellotti, R.;
- Sassi, M. P.; Žel, J., Droplet volume variability as a critical factor for accuracy of absolute
- quantification using droplet digital PCR. Anal. Bioanal. Chem. 2017, 409 (28), 6689-6697.
- 504 39. Tice, J. D.; Lyon, A. D.; Ismagilov, R. F., Effects of viscosity on droplet formation and
- mixing in microfluidic channels. Anal. Chim. Acta 2004, 507 (1), 73-77.
- 506 40. Teo, A. J.; Li, K.-H. H.; Nguyen, N.-T.; Guo, W.; Heere, N.; Xi, H.-D.; Tsao, C.-W.;
- Li, W.; Tan, S. H., Negative pressure induced droplet generation in a microfluidic flow-focusing
- 508 device. Anal. Chem. 2017, 89 (8), 4387-4391.
- 509 41. Zeng, W.; Yang, S.; Liu, Y.; Yang, T.; Tong, Z.; Shan, X.; Fu, H., Precise
- monodisperse droplet generation by pressure-driven microfluidic flows. Chem. Eng. Sci. 2022,
- 511 *248*, 117206.
- 512 42. Fontenot, K.; Schork, F. J., Sensitivities of droplet size and stability in monomeric
- 513 emulsions. *Ind. Eng. Chem. Res.* **1993,** *32* (2), 373-385.

- Mori, Y.; Nagamine, K.; Tomita, N.; Notomi, T., Detection of loop-mediated isothermal
- amplification reaction by turbidity derived from magnesium pyrophosphate formation. *Biochem*.
- 516 Biophys. Res. Commun. 2001, 289 (1), 150-154.
- 44. Gadkar, V. J.; Goldfarb, D. M.; Gantt, S; Tilley, P. A., Real-time detection and monitoring of
- loop mediated amplification (LAMP) reaction using self-quenching and de-quenching fluorogenic
- 519 probes. Sci. Rep. 2018, 8 (1), 1-10.
- 520 45. Ding, S.; Chen, G.; Wei, Y.; Dong, J.; Du, F.; Cui, X.; Huang, X.; Tang, Z., Sequence-
- 521 specific and multiplex detection of COVID-19 virus (SARS-CoV-2) using proofreading enzyme-
- mediated probe cleavage coupled with isothermal amplification. *Biosens. Bioelectron.*, **2021**, 178,
- 523 113041.

525

526

527

528

529

530

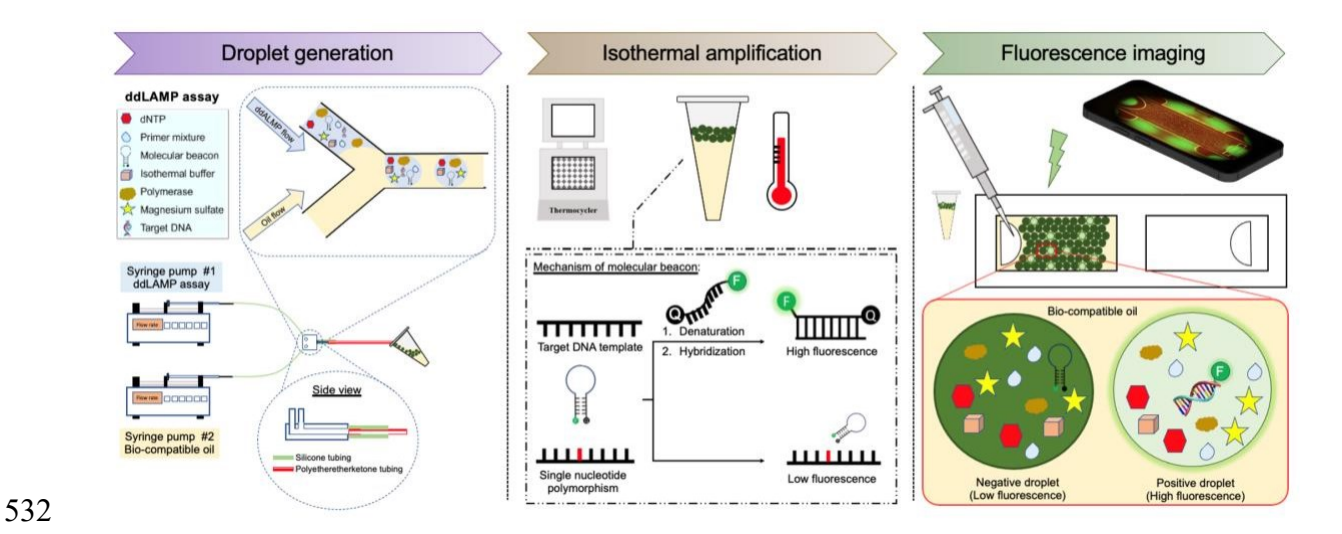


Figure 1. Methods for performing ddLAMP using an assay featuring MB as a sequence-specific probe for SNP detection. Droplet generation (left) is facilitated by a 3D printed generator with 2 syringe pumps. Isothermal amplification (center) results in enhanced fluorescence of the target sequence due to selective annealing with the MB. Droplets are imaged (right) on counting slides with a fluorescence microscope equipped with a EGFP filter and/or with a smartphone-based imaging system.

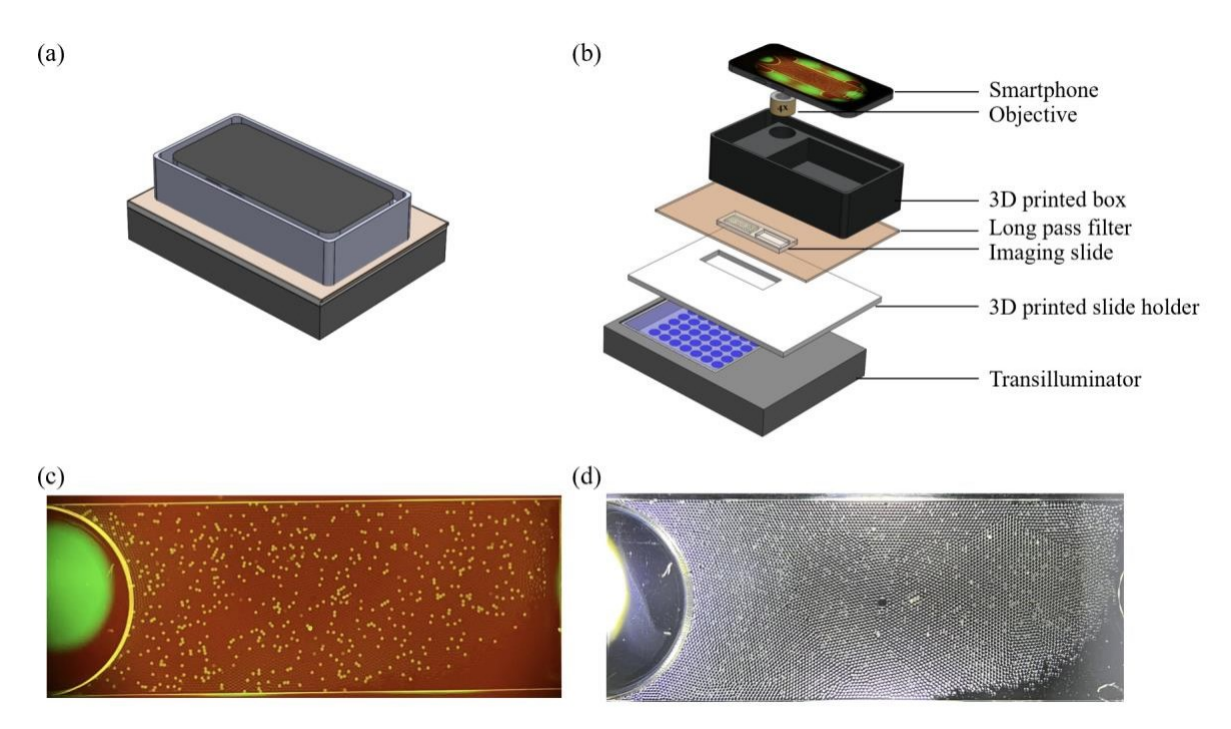


Figure 2. Schematic of the (a) smartphone-based imaging system and (b) all components including a smartphone, objective, 3D printed box, long pass filter, imaging slide, 3D printed slide holder, and transilluminator. Fluorescence (c) and brightfield (d) images of the ddLAMP assay taken using the smartphone system are shown.

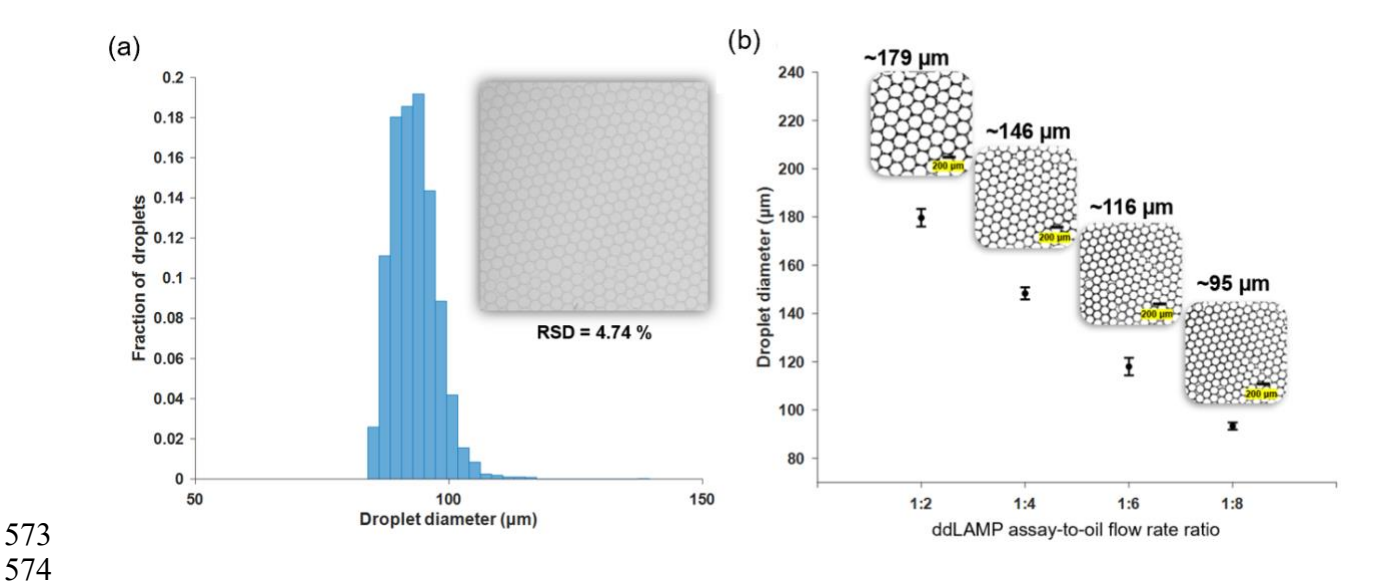


Figure 3. Droplet sizes formed by 3D printed droplet generation system using ddLAMP assay. (a) Droplet diameter distribution of ddLAMP assay and (b) effect of ddLAMP assay-to-oil flow rate ratio on droplet diameter. All ddLAMP assays were subjected to isothermal amplification at 65 °C for 60 minutes and contained 1.4 mM dNTPs, 6 mM MgSO₄, isothermal amplification buffer (1X), 1.6 μM FIP, 1.6 μM BIP, 0.2 μM F3, 0.2 μM B3, 0.4 μM LF, 0.7 μM MB, 0.32 U/μL *Bst* 2.0 WarmStart DNA polymerase, and 5 μL OmpW DNA template.

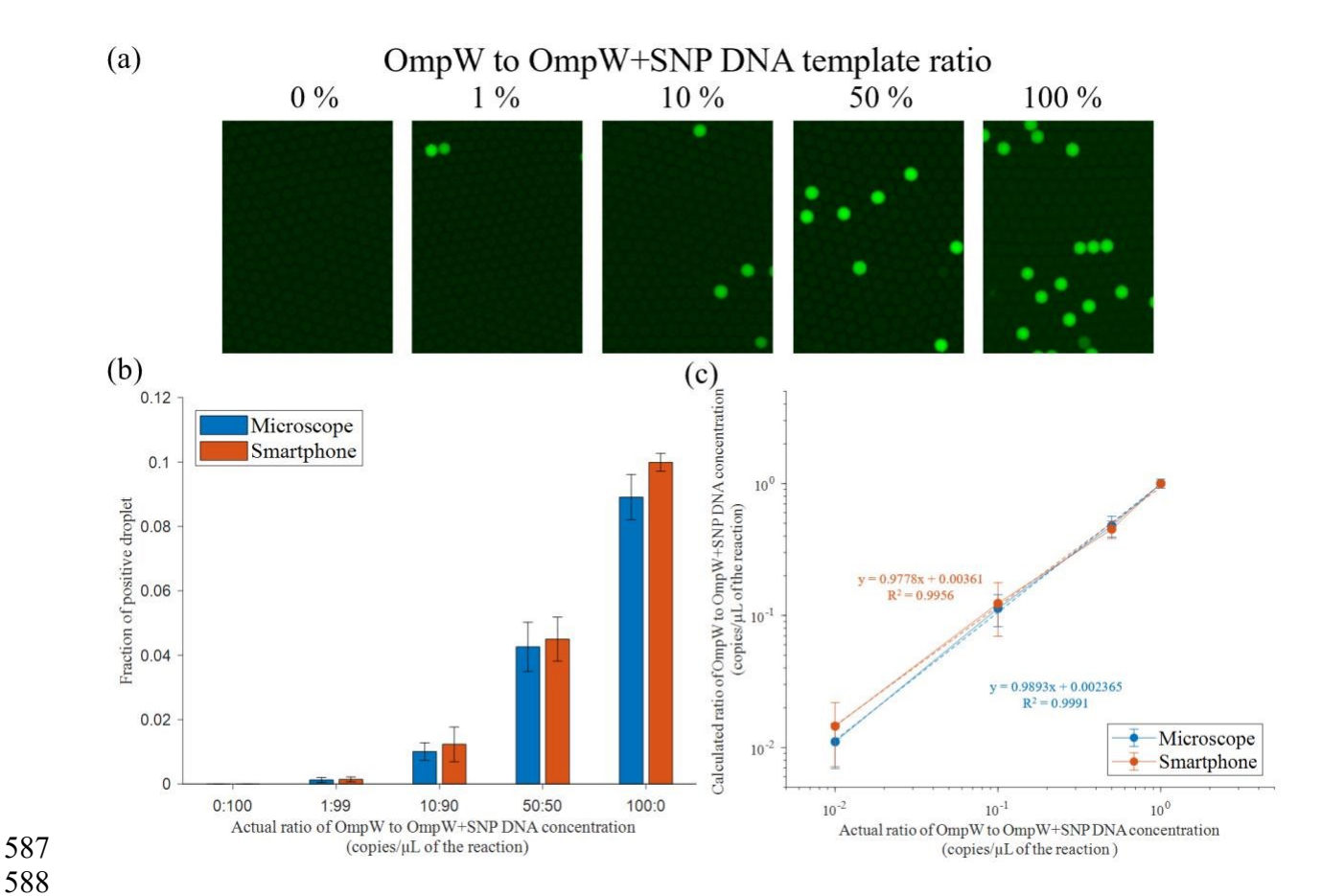


Figure 4. Statistical analysis of MB-ddLAMP by applying various copy ratios of OmpW to OmpW+SNP DNA template at 0:100, 1:99, 10:90, 50:50, 100:0. Panel (a) shows fluorescent droplet images obtained by microscopy. Plots in (b) describe the relationship between fraction of positive droplets versus ratio of OmpW to OmpW+SNP DNA template using fluorescence microscopy and smartphone imaging and (c) the relationship between calculated versus actual ratio of OmpW to OmpW+SNP DNA template.

TOC image

